Topological quantum phase transition between Fermi liquid phases in an Anderson impurity model

G. G. Blesio and L. O. Manuel
Instituto de Física Rosario (CONICET) and Universidad Nacional de Rosario, Bv. 27 de Febrero 210 bis, 2000 Rosario, Argentina

P. Roura-Bas and A. A. Aligia
Centro Atómico Bariloche and Instituto Balseiro, Comisión Nacional de Energía Atómica, CONICET, 8400 Bariloche, Argentina

(Received 4 June 2018; revised manuscript received 19 September 2018; published 26 November 2018)

We study a generalized Anderson model that mixes two localized configurations—one formed by two degenerate doublets and the other by a triplet with single-ion anisotropy DS_z^2—by means of two degenerate conduction channels. The model has been derived for a single Ni impurity embedded into an O-doped Au chain. Using the numerical renormalization group, we find a topological quantum phase transition, at a finite value D_c, between two regular Fermi liquid phases of high (low) conductance and topological number $2I_L/\pi = 0$ $(+1)$ for $D < D_c$ $(D > D_c)$, where I_L is the well-known Luttinger integral. At finite temperature the two phases are separated by a non-Fermi liquid phase with fractional impurity entropy $\frac{1}{2}\ln 2$ and other properties which are similar to those of the two-channel Kondo model.

DOI: 10.1103/PhysRevB.98.195435

Introduction. Quantum phase transitions (QPTs) observed in transport through molecular systems in which two electrons play a relevant role have been a subject of interest recently [1–3]. In general, in nanoscopic systems with more than one electron, the spin-orbit coupling is important and leads to the single-ion anisotropy DS_z^2, where S_z is the total spin of the nanosystem [2–6]. The relative magnitude of D can be tuned experimentally [2,6–8]. On the other hand, experiments with mechanically controllable break junctions have made it possible to create one-dimensional atomic chains of several elements and measure the conductance through them [9,10].

Some QPTs are topological QPTs (TQPTs): Even if some other properties vary continuously at the transition, a topological quantum number (related with a geometrical Berry phase or the topology of each thermodynamic phase) jumps at the TQPT. Examples of these kinds of transitions are several charge and spin TQPTs observed in one-dimensional models in which the nearest-neighbor hopping depends on the occupation [11,12], as in cold-atom lattices [13], or the Hubbard model with alternative on-site energies [14,15], for which the topological transition might be observable in transport through arrays of quantum dots or molecules [16].

On the other hand, in condensed matter physics, the Luttinger theorem [17,18], which states that the volume of the Fermi surface is determined by the particle density and remains unaltered by interactions, and Friedel sum rules [19,20], which relate the occupancy of impurity states with the corresponding spectral density at the Fermi energy, have been crucial for our present understanding of many interacting systems that behave as Fermi liquids at zero temperature. The so-called Luttinger integral I_L [21] enters the demonstrations in these works and it was generally assumed to vanish. In non-Fermi liquid phases, it has been found that I_L can take nontrivial values [22,23]. However, recently a group of researchers found that I_L can take three different values in an impurity model in phases with regular low-energy Fermi liquid behavior [24,25]. This is surprising since only $I_L = 0$ was expected in a regular Fermi liquid, according to its perturbative calculation in the seminal work by Luttinger and Ward [18], where the Fermi liquid was considered adiabatically connected to a system of noninteracting electrons. More recently, Seki and Yunoki [26] showed that the Luttinger integral, which is the deviation of the Luttinger volume from the noninteracting limit, can be interpreted as a winding number of the ratio between the determinants of the noninteracting and interacting single-particle Green's functions. The combination of this topological interpretation of I_L and the finding of its nonzero values [24,25] opens the possibility of topologically nontrivial Fermi liquid phases that are not adiabatically connected with noninteracting systems and, therefore, they can be termed *non-Landau* Fermi liquids.

In this work, we describe the TQPT that, driven by the single-ion anisotropy D, takes place in a simple impurity model which, in the Kondo limit, consists of a spin 1 screened by two conduction channels. This model has been derived from *ab initio* calculations and describes transport through Ni atoms in O-doped Au chains [27,28] (see Supplemental Fig. S1 of Ref. [29]). The oxygen doping has the effect of pushing up the $5d_{xz}$ and $5d_{yz}$ bands of Au (with z along the chain direction), which are below the Fermi energy in pure Au chains [28,35,36]. The two conduction channels correspond to the degenerate orbitals of xz and yz symmetry, and they hybridize with the corresponding Ni $3d$ orbitals. Solving the model by means of the numerical renormalization group (NRG), we find that the transition occurs at the finite critical anisotropy $D_c \approx 2.57\ T_K^0$, where T_K^0 is the Kondo temperature for $D = 0$. This TQPT separates two regular Fermi liquid phases: For $D < D_c$ the impurity spin is Kondo screened, while for $D > D_c$ it is quenched by the anisotropy. For $D < D_c$, as the temperature $T \to 0$, the electrical

conductance is large and agrees with the usual Friedel sum rule with $I_L = 0$, as in Fermi liquids adiabatically connected with a noninteracting system. Instead, for $D > D_c$ and $T = 0$, the conductance is small and satisfies a generalized Friedel sum rule with $I_L = \frac{\pi}{2}$, corresponding to a *non-Landau* Fermi liquid. Furthermore, for $D \approx D_c$ and in a finite interval of temperatures $T^*(D) \leqslant T \lesssim T_K^0$, where $T^*(D) \to 0$ as $D \to D_c$ [37], there is a critical quantum regime whose electrical transport and thermodynamics properties correspond to a non-Fermi liquid behavior. It is worthwhile to mention that T_K^0 can be tuned by stretching the gold chains, rendering it possible to observe the transition experimentally.

Model. We consider the Hamiltonian that describes a system containing a Ni atom in a substitutional position within a Au chain doped with a small amount of oxygen (∼14%) between two Au conducting leads [27,28], describing charge fluctuations between $3d^8$ and $3d^9$ Ni configurations. It can be written as [29]

$$\begin{aligned} H = &\sum_{M_2} \left(E_2 + D M_2^2\right) |M_2\rangle\langle M_2| + \sum_{\alpha M_1} E_1 |\alpha M_1\rangle\langle \alpha M_1| \\ &+ \sum_{\nu k \alpha \sigma} \varepsilon_{\nu k} c^\dagger_{\nu k \alpha \sigma} c_{\nu k \alpha \sigma} \\ &+ \sum_{\substack{M_1 M_2 \\ \alpha \nu k \sigma}} V_\nu \langle 1 M_2 | \tfrac{1}{2}\tfrac{1}{2} M_1 \sigma\rangle (|M_2\rangle\langle \alpha M_1| c_{\nu k \alpha \sigma} + \text{H.c.}), \end{aligned} \tag{1}$$

where E_i and M_i indicate the energies and the spin projections along the chain, respectively, of states with $i = 1, 2$ holes in the $3d$ shell of the Ni impurity; $|\alpha M_1\rangle$ is the state with one hole with symmetry α (xz, yz) and spin M_1. D is the Ni uniaxial magnetic anisotropy. The operator $c^\dagger_{\nu k \alpha \sigma}$ creates a hole with symmetry α and energy $\varepsilon_{\nu k}$ (relative to the Fermi level $\varepsilon_F = 0$) in the $5d$ shell of the Au atom, where $\nu = L, R$ denotes the left or the right side of the Ni atom, respectively. $\langle 1 M_2 | \frac{1}{2}\frac{1}{2} M_1 \sigma\rangle$ are Clebsh-Gordan coefficients. The hopping V_ν characterizes the tunneling between the Ni and Au states, and it enters the hybridization function $\Delta = \pi \sum_{\nu k} |V_\nu|^2 \delta(\omega - \varepsilon_{\nu k})$, assumed independent of energy.

The ground-state configuration of the Ni atom has two holes in the degenerate $3d_{xz}$, $3d_{yz}$ orbitals coupled to spin $S = 1$. The state $|M_2\rangle$ with $M_2 = 0$ is lower in energy than those with $M_2 = \pm 1$ by an energy that has been estimated in $D \approx 8.5$ meV solving exactly the atomic model for the $3d^8$ configuration including all interactions and spin-orbit coupling [27].

We solve the Hamiltonian (1) by means of NRG, as implemented in the Ljubljana open source code [38]. We use a discretization parameter $\Lambda = 3$, and we keep up to 10 000 states. The results are z averaged with N_z up to 4. In this work, we have chosen $\varepsilon_d \equiv E_2 - E_1 = -0.02$ and $\Delta = 0.1$ in units of the conduction half-bandwidth W. For this ratio ε_d/Δ, the system is in the Kondo regime, but close to the mixed valence regime (MVR), and the different regimes that we want to display come out more clearly. The corresponding Kondo temperature is $T_K^0 \simeq 1.245 \times 10^{-3}$ for $D = 0$, obtained through the usual condition $G(T_K^0) = \frac{1}{2} G(T \to 0)$, where $G(T)$ is the differential conductance $G = dI/dV$. However, the occupancy found in *ab initio* calculations [27,28] indicates that the system is closer to the MVR and with a Kondo temperature near 6 meV, as explained in the Supplemental Material [29]. The corresponding value $D_c \simeq 2.57 T_K^0 \sim 15$ meV roughly falls in the range of the estimated D for Ni atoms in O-doped Au chains, particularly taking into account that D can be reduced by stretching or tuned by further doping the gold chains.

Generalized Friedel sum rule. Using conservation laws, the impurity spectral function per orbital and spin, at the Fermi level and $T = 0$, is given by [20]

$$A_{d\alpha\sigma}(\omega = 0) = \frac{1}{\pi \Delta} \sin^2(\delta_{\alpha\sigma}), \tag{2}$$

where, taking into account explicitly the spin degeneracy, the phase shift is

$$\delta_{\alpha\sigma} = \frac{\pi}{2} \langle n_{d\alpha}\rangle - I_L. \tag{3}$$

$n_{d\alpha} = \sum_{M_2} |M_2\rangle\langle M_2| + \sum_{M_1} |\alpha M_1\rangle\langle \alpha M_1|$ is the hole occupation number of the Ni α orbital [39], and the Luttinger integral I_L, which in our case is independent of orbital and spin indices, is defined as [21]

$$I_L = \text{Im} \int_{-\infty}^{0} d\omega G_{d\alpha\sigma}(\omega) \frac{\partial \Sigma_{d\alpha\sigma}(\omega)}{\partial \omega}, \tag{4}$$

where $G_{d\alpha\sigma}(\omega)$ is the impurity Green function for orbital α and spin σ and $\Sigma_{d\alpha\sigma}(\omega)$ is the corresponding self-energy.

As explained above, I_L vanishes for a Fermi liquid, when it is perturbatively calculated from a noninteracting electronic system [18]. However, recently [24,25] it was found that this is not always the case for local Fermi liquids, while a topological interpretation of I_L was provided for extended systems [26].

NRG results. To localize the TQPT we use the differential conductance, which is easily accessible experimentally [9,10]. The conductance per channel is given by

$$G_\alpha(T) = G_0 \sum_\sigma \frac{\pi \Delta}{2} \int d\omega \left[-\frac{\partial f(\omega)}{\partial \omega}\right] A_{d\alpha\sigma}(\omega), \tag{5}$$

where $f(\omega)$ is the Fermi function and $G_0 = 2e^2/h$ is the quantum of conductance. Using Eqs. (2) and (3) we have, at zero temperature, the generalized Friedel sum rule for the conductance

$$G_\alpha(0) = G_0 \sin^2\left(\frac{\pi}{2} \langle n_{d\alpha}\rangle - I_L\right). \tag{6}$$

In Fig. 1, the conductance per channel as a function of T/T_K^0 for several positive values of the single-ion anisotropy D is shown. G_α has an abrupt change as D is varied across its critical value $D_c \simeq 0.003196$, and two regimes are easily characterized according to the behavior of G_α at the lowest temperatures. For $D < D_c$, $G_\alpha(T \to 0)$ takes a large value, which corresponds to the Friedel sum rule (6) with $I_L = 0$. In this case, for low temperatures we expect a fully Kondo screened impurity, leading to the usual Fermi liquid phase. Note that, as we are working far away from the particle-hole symmetric point (only $3d^8$ and $3d^9$ Ni configurations are considered), the occupation number per impurity orbital

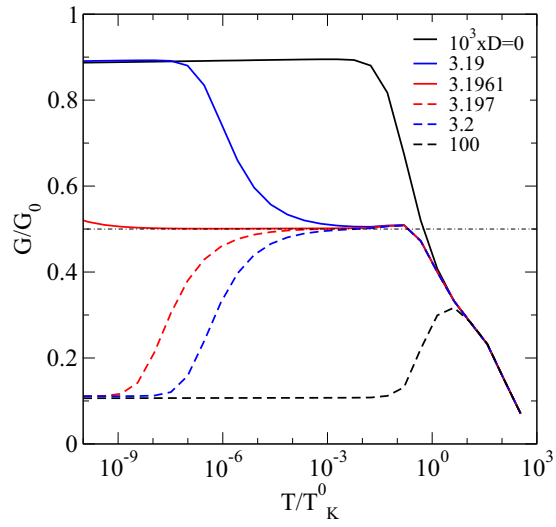

FIG. 1. Electrical differential conductance as a function of T/T_K^0 for several values of the single-ion anisotropy D.

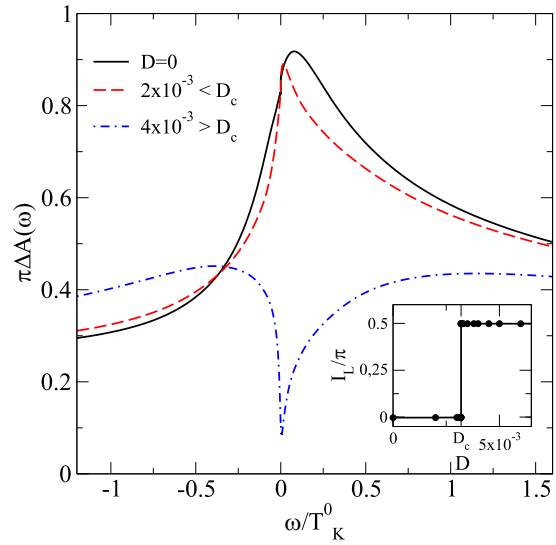

FIG. 2. Impurity spectral function $A_{d\alpha\sigma}(\omega)$ for three different anisotropies D, at $T \simeq 10^{-6}T_K^0$. Inset: Luttinger integral I_L as a function of D.

is less than 1 ($\langle n_{d\alpha}\rangle \simeq 0.788$, almost constant with varying D) and G_α does not reach the unitary limit. It can be seen that, for small D, the conductance exhibits fingerprints of the magnetic anisotropy for temperatures of the order of D, like the shoulder that develops before it goes to its Kondo limit with decreasing T.

On the other hand, for $D > D_c$, $G_\alpha(T \to 0)$ goes to a low value, corresponding to $I_L = \frac{\pi}{2}$ in (6). This case corresponds to the impurity spin quenched by D, as its ground state has spin projection $S_z = 0$. Again, we expect a Fermi liquid at low T, but now this phase yields the nontrivial Luttinger integral $I_L = \frac{\pi}{2}$. For $D \gg D_c$, G_α takes small values for any temperature.

For D close to D_c, below and above, the conductance has a clear plateau at the precise value $G_0/2$, characteristic of the two-channel Kondo (2CK) effect.

Around D_c we define a characteristic energy for each phase. For $D < D_c$, $T_K^*(D)$ is computed through the condition $G_\alpha[T_K^*(D)] = [G_\alpha(T \to 0) - 0.5G_0]/2$, corresponding to the onset of the fully Kondo screening of the impurity, while for $D > D_c$, we take $T_q^*(D)$ which satisfies $G_\alpha[T_q^*(D)] = [0.5G_0 - G_\alpha(T \to 0)]/2$, and it signals the onset of the impurity spin quenching. We find that, as it corresponds to a quantum critical point [37], these energies vanish as $D \to D_c$. Surprisingly for a Kondo screening energy scale, $T_K^*(D)$ has a potential law dependence on D:

$$T_K^*(D) \propto T_K^0 \left(\frac{D_c - D}{D_c}\right)^2.$$

On the other hand,

$$T_q^*(D) \propto T_K^0 \exp\left[-c\left(\frac{T_K^0}{D - D_c}\right)^{1/4}\right],$$

where c is a constant of order of one; a similar result was found in the $S = 1$ underscreened Kondo model [40].

The impurity spectral function $A_{d\alpha\sigma}(\omega)$ near the Fermi level is presented in the main panel of Fig. 2, for three different values of D, at the very low temperature $T \simeq 10^{-6}T_K^0$. A Kondo resonance is clearly visible for all $D < D_c$. As D increases, the Kondo peak moves towards the Fermi level and its width decreases. At D_c the resonance abruptly disappears, and it is replaced by a narrow dip just at $\omega = 0$. In the supplemental material [29], we show that for the related $S = 1$ Kondo impurity model with two conduction channels, very close to its critical point, the spectral function (defined through the t matrix) takes half of its Kondo-screened value, and this is another hallmark of the 2CK.

With the NRG technique it is not an easy task to obtain reliable values of I_L by computing it directly from Eq. (4), due to numerical inaccuracies in the self-energy evaluation [24]. Instead, we calculate I_L through the generalized Friedel sum rule for the conductance (6). The obtained I_L is displayed as a function of D in the inset of Fig. 2. It can be seen that I_L takes only two discrete values: $I_L = 0, \pi/2$, with an abrupt jump at D_c. This is not fortuitous as I_L is closely related with the winding number of the ratio $D_d(z) = G^0_{d\alpha\sigma}(z)/G_{d\alpha\sigma}(z)$ between the noninteracting and interacting impurity Green's functions, around the origin in the complex plane D_d (see supplemental material [29]):

$$I_L = \pi \lim_{T\to 0} \oint_\Gamma \frac{dz}{2\pi i} n_F(z) \frac{\partial \ln D_d(z)}{\partial z}, \tag{7}$$

where the contour Γ encloses the real axis. So, the Fermi liquids for $D < D_c$ and $D > D_c$ can be topologically distinguished by I_L, being topologically trivial (non-trivial) synonymous of adiabatically (non-adiabatically) connected to a noninteracting system. As a consequence, the quantum critical transition between the two Fermi liquids (a *Landau* and a *non-Landau* Fermi liquid) at D_c has a topological character. We confirm the Fermi liquid character of both phases through the analysis of their NRG spectra, that point out that for $D < D_c$ ($D > D_c$) the Fermi liquid, corresponds to a strong-coupling (weak-coupling) fixed point [29]. Furthermore, with the necessary caution due to the difficulties of the NRG

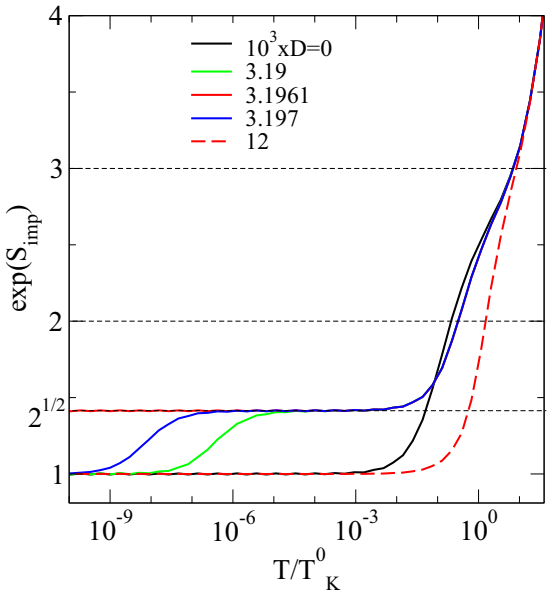

FIG. 3. Impurity entropy as a function of temperature for several single-ion anisotropy D close to the TQPT.

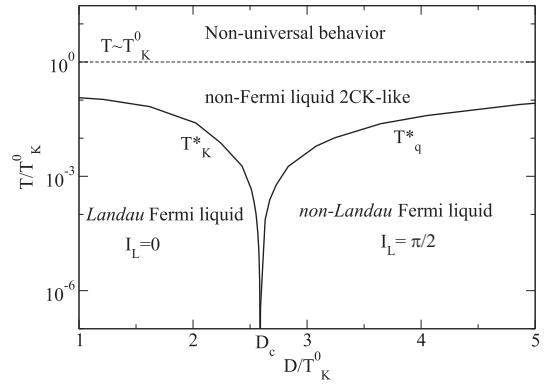

FIG. 4. Sketch of the phase diagram of the $S = 1$ impurity model as a function of temperature and anisotropy. The solid lines indicate crossover regions between Fermi and non-Fermi liquid behaviors, while the dashed one signals the onset of nonuniversal behavior at higher temperatures.

computation of the self-energy [29,41], we have checked that its imaginary part Im $\Sigma_{d\alpha\sigma}(\omega)$ behaves quadratically as a function of frequency close to the Fermi level, for both Fermi liquids $I_L = 0, \pi/2$ [29]. However, for $D \simeq D_c$ a singularity appears just on the Fermi level, being responsible for the nontrivial I_L. We conjecture that this singularity is related with the simultaneous creation, as $D \to D_c$ from below, of a zero and a pole of the impurity Green's function at the Fermi level, as it happens in an analogous way in other topological transitions in extended systems [42,43].

In order to further characterize the critical region, the impurity contribution to the entropy as a function of temperature is plotted in Fig. 3. It can be clearly seen that, for D close to D_c, there is a plateau at $S_{\rm imp} = \frac{1}{2}\ln(2)$, the fractional entropy usually associated with the 2CK physics [44]. Also, a shoulder at $S \simeq 3$ is noticeable, corresponding to the threefold degeneracy of the $S = 1$ impurity states at intermediate temperature. For other parameters (not shown in this work), this shoulder transforms in a clear plateau. At higher temperatures, out of the figure, there is a plateau at $S_{\rm imp} = 7$ corresponding to the total number of localized impurity states in the model.

Another signature of 2CK-like behavior close to D_c is the fact that the NRG spectrum, as a function of the NRG iteration number N (see supplemental material [29]), has an extended plateau for intermediate N, corresponding to a (unstable) fixed point without the typical odd-even alternation and uniform level spacing of the conventional Kondo effect [45].

Using the energy scales T_K^* and T_q^*, we can summarize our findings in the phase diagram sketched in Fig. 4, with its "classical" Fermi liquid regions at both sides of the critical point, while the usual (non-Fermi liquid) quantum critical wedge emerges from the quantum critical point D_c at zero temperature.

Summary. We have found a topological quantum phase transition between two Fermi liquids through an intermediate non-Fermi liquid 2CK-like phase in a simple model consisting of an $S = 1$ impurity coupled to two conduction bands, where the driving parameter of the transition is the single-ion magnetic anisotropy D. This model has experimental relevance for transport through nanostructures formed by Ni impurities in O-doped gold chains. The relative magnitude of anisotropy to the Kondo temperature T_K^0 can be experimentally tunable, rendering it possible to observe the transition: D/T_K^0 can be modified by changing the effective ε_d of the Ni atom by doping or it can be increased by mechanically streching the gold chains [2]. We expect that our work will stimulate further experimental work in similar systems. In particular, it would be interesting to find experimental probes that can distinguish between Fermi liquids characterized by different values of the topological invariant Luttinger integral.

Acknowledgements. We acknowledge financial support provided by PIP 112-201501-00506 of CONICET (Argentina) and PICT 2013-1045 of the ANPCyT (Argentina).

[1] N. Roch, S. Florens, V. Bouchiat, W. Wernsdorfer, and F. Balestro, Quantum phase transition in a single-molecule quantum dot, Nature (London) **453**, 633 (2008).

[2] J. J. Parks, A. R. Champagne, T. A. Costi, W. W. Shum, A. N. Pasupathy, E. Neuscamman, S. Flores-Torres, P. S. Cornaglia, A. A. Aligia, C. A. Balseiro, G. K.-L. Chan, H. D. Abruña, and D. C. Ralph, Mechanical control of spin states in spin-1 molecules and the underscreened Kondo effect, Science **328**, 1370 (2010).

[3] For a review see S. Florens, A. Freyn, N. Roch, W. Wernsdorfer, F. Balestro, P. Roura-Bas, and A. A. Aligia, Universal transport signatures in two-electron molecular quantum dots: Gate-tunable Hund's rule, underscreened Kondo effect and quantum phase transitions, J. Phys.: Condens. Matter **23**, 243202 (2011); references therein.

[4] G. Katsaros, P. Spathis, M. Stoffel, F. Fournel, M. Mongillo, V. Bouchiat, F. Lefloch, A. Rastelli, O. G. Schmidt, and S. De Franceschi, Hybrid superconductorsemiconductor devices

made from self-assembled SiGe nanocrystals on silicon, Nat. Nanotechnol. **5**, 458 (2010).

[5] T. S. Jespersen, K. Grove-Rasmussen, J. Paaske, K. Muraki, T. Fujisawa, J. Nygard, and K. Flensberg, Gate-dependent spin-orbit coupling in multielectron carbon nanotubes, Nat. Phys. **7**, 348 (2011).

[6] R. Hiraoka, E. Minamitani, R. Arafune, N. Tsukahara, S. Watanabe, M. Kawai, and N. Takagi, Single-molecule quantum dot as a Kondo simulator, Nat. Commun. **8**, 16012 (2017).

[7] J. C. Oberg, M. R. Calvo, F. Delgado, M. Moro-Lagares, D. Serrate, D. Jacob, J. Fernandez-Rossier, and C. F. Hirjibehedin, Control of single-spin magnetic anisotropy by exchange coupling, Nat. Nanotechnol. **9**, 64 (2013).

[8] B. W. Heinrich, L. Braun, J. I. Pascual, and K. J. Franke, Tuning the magnetic anisotropy of single molecules, Nano Lett. **15**, 4024 (2015).

[9] H. Ohnishi, Y. Kondo, and K. Takayanagi, Quantized conductance through individual rows of suspended gold atoms, Nature **395**, 780 (1998).

[10] V. Rodrigues, J. Bettini, P. C. Silva, and D. Ugarte, Evidence for Spontaneous Spin-Polarized Transport in Magnetic Nanowires, Phys. Rev. Lett. **91**, 096801 (2003).

[11] A. A. Aligia, K. Hallberg, C. D. Batista and G. Ortiz, Phase diagrams from topological transitions: The Hubbard chain with correlated hopping, Phys. Rev. B **61**, 7883 (2000).

[12] A. A. Aligia, A. Anfossi, L. Arrachea, C. Degli Esposti Boschi, A. O. Dobry, C. Gazza, A. Montorsi, F. Ortolani, and M. E. Torio, Incommmensurability and Unconventional Superconductor to Insulator Transition in the Hubbard Model with Bond-Charge Interaction, Phys. Rev. Lett. **99**, 206401 (2007).

[13] L.-M. Duan, Effective Hamiltonian for Fermions in an Optical Lattice Across a Feshbach Resonance, Phys. Rev. Lett. **95**, 243202 (2005); General Hubbard Model for Strongly Interacting Fermions in an Optical Lattice and its Phase Detection, Europhys. Lett. **81**, 20001 (2008).

[14] M. Fabrizio, A. O. Gogolin, and A. A. Nersesyan, From Band Insulator to Mott Insulator in One Dimension, Phys. Rev. Lett. **83**, 2014 (1999).

[15] M. E. Torio, A. A. Aligia, and H. A. Ceccatto, Phase diagram of the Hubbard chain with two atoms per cell, Phys. Rev. B **64**, 121105(R) (2001).

[16] A. A. Aligia, K. Hallberg, B. Normand, and A. P. Kampf, Detection of Topological Transitions by Transport Through Molecules and Nanodevices, Phys. Rev. Lett. **93**, 076801 (2004).

[17] J. M. Luttinger, Fermi surface and some simple equilibrium properties of a system of interacting fermions, Phys. Rev. **119**, 1153 (1960).

[18] J. M. Luttinger and J. C. Ward, Ground-state energy of a many-fermion system. II, Phys. Rev. **118**, 1417 (1960).

[19] D. C. Langreth, Friedel sum rule for Anderson's model of localized impurity states, Phys. Rev. **150**, 516 (1966).

[20] A. Yoshimori and A. Zawadowski, Restricted Friedel sum rules and Korringa relations as consequences of conservation laws, J. Phys. C **15**, 5241 (1982).

[21] The integral I_L is in Eq. (63) of Ref. [18], Eq. (23) of Ref. [19], and Eq. (3.3) of Ref. [20]. In our case it is given by Eq. (4).

[22] D. E. Logan, C. J. Wright, and M. R. Galpin, Correlated electron physics in two-level quantum dots: Phase transitions, transport, and experiment, Phys. Rev. B **80**, 125117 (2009).

[23] A. K. Mitchell, D. E. Logan, and H. R. Krishnamurthy, Two-channel Kondo physics in odd impurity chains, Phys. Rev. B **84**, 035119 (2011).

[24] O. J. Curtin, Y. Nishikawa, A. C. Hewson, and D. J. G. Crow, Fermi liquids and the Luttinger theorem, J. Phys. Commun. **2**, 031001 (2018).

[25] Y. Nishikawa, O. J. Curtin, A. C. Hewson, and D. J. G. Crow, Magnetic field induced quantum criticality and the Luttinger sum rule, Phys. Rev. B **98**, 104419 (2018).

[26] K. Seki and S. Yunoki, Topological interpretation of the Luttinger theorem, Phys. Rev. B **96**, 085124 (2017).

[27] S. Di Napoli, M. A. Barral, P. Roura-Bas, L. O. Manuel, A. M. Llois, and A. A. Aligia, Kondo physics in a Ni impurity embedded in O-doped Au chains, Phys. Rev. B **92**, 085120 (2015).

[28] M. A. Barral, S. Di Napoli, G. Blesio, P. Roura-Bas, A. Camjayi, L. O. Manuel, and A. A. Aligia, Kondo behavior and conductance through 3d impurities in gold chains doped with oxygen, J. Chem. Phys. **146**, 092315 (2017).

[29] See Supplemental Material at http://link.aps.org/supplemental/10.1103/PhysRevB.98.195435 for details about the NRG calculations, the estimation of realistic parameters of the impurity model, results on the $S = 1$ Kondo impurity coupled to two conduction bands, and the topological interpretation of the Luttinger integral. Supplemental material includes Refs. [30–34].

[30] M. Núñez, D. C. Freitas, F. Gay, J. Marcus, P. Strobel, A. A. Aligia, and M. Núñez-Regueiro, Orbital Kondo effect in V-doped 1T-$CrSe_2$, Phys. Rev. B **88**, 245129 (2013).

[31] G. G. Blesio, L. O. Manuel, A. A. Aligia, and P. Roura-Bas (unpublished).

[32] A. C. Hewson, *The Kondo Problem to Heavy Fermions* (Cambridge University Press, Cambridge, UK, 1997).

[33] R. Bulla, A. C. Hewson, and T. Pruschke, Numerical renormalization group calculations for the self-energy of the impurity Anderson model, J. Phys.: Condens. Matter **10**, 8365 (1998).

[34] A. K. Mitchell and D. E. Logan, Two-channel Kondo phases and frustration-induced transitions in triple quantum dots, Phys. Rev. B **81**, 075126 (2010).

[35] W. H. A. Thijssen, D. Marjenburgh, R. H. Bremmer, and J. M. van Ruitenbeek, Oxygen-Enhanced Atomic Chain Formation, Phys. Rev. Lett. **96**, 026806 (2006).

[36] S. Di Napoli, A. Thiess, S. Blügel, and Y. Mokrousov, Modelling impurity-assisted chain creation in noble-metal break junctions, J. Phys.: Condens. Matter **24**, 135501 (2012).

[37] Y. Nishikawa, D. J. G. Crow, and A. C. Hewson, Convergence of Energy Scales on the Approach to a Local Quantum Critical Point, Phys. Rev. Lett. **108**, 056402 (2012).

[38] R. Žitko, NRG Ljubljana—open source numerical renormalization group code [http://nrgljubljana.ijs.si].

[39] In general, $\langle n_{d\alpha}\rangle$ in Eq. (3) includes also the change in the occupancy of conduction electrons due to the hybridization with the impurity [19], but this term vanishes for a wide flat conduction band as we assume in our numerical calculations. This assumption does not affect any of our main results.

[40] P. S. Cornaglia, P. Roura Bas, A. A. Aligia and C. A. Balseiro, Quantum transport through a stretched spin-1 molecule, Europhys. Lett. **93**, 47005 (2011).

[41] R. Žitko (private communication).

[42] S. Sakai, Y. Motome, and M. Imada, Evolution of Electronic Structure of Doped Mott Insulators: Reconstruction of Poles and Zeros of Green's Function, Phys. Rev. Lett. **102**, 056404 (2009).

[43] V. Gurarie, Single-particle Green's functions and interacting topological insulators, Phys. Rev. B **83**, 085426 (2011).

[44] A. K. Mitchell, E. Sela, and D. E. Logan, Two-Channel Kondo Physics in Two-Impurity Kondo Models, Phys. Rev. Lett. **108**, 086405 (2012).

[45] H. B. Pang and D. L. Cox, Stability of the fixed point of the two-channel Kondo Hamiltonian, Phys. Rev. B **44**, 9454 (1991).